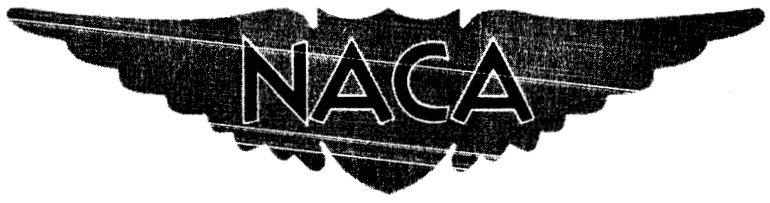


# RESEARCH MEMORANDUM

## EFFECT OF PRESSURE LEVEL ON AFTERBURNER-WALL TEMPERATURES

By Thomas B. Shillito and George R. Smolak

Lewis Flight Propulsion Laboratory
Cleveland, Ohio







NATIONAL ADVISORY COMMITTEE
FOR AERONAUTICS

WASHINGTON

June 11, 1958

NATIONAL ADVISORY COMMITTEE FOR AERONAUTICS

RESEARCH MEMORANDUM

# EFFECT OF PRESSURE LEVEL ON AFTERBURNER-WALL TEMPERATURES

By Thomas B. Shillito and George R. Smolak

## SUMMARY

An investigation was conducted on a full-scale afterburner and turbojet engine to determine the effect of pressure level on afterburner-wall temperature. The investigation was prompted by speculation that luminous radiation from nongaseous substances in the afterburner gas stream might be present and might vary significantly with pressure.

Afterburner-outlet pressures from 3700 to 6500 pounds per square foot absolute were investigated. For a given ratio of cooling airflow to afterburner gas flow, the afterburner-wall temperature increased as afterburner-outlet pressure was increased. This increasing wall temperature was due to the increasing local gas temperatures near the wall and not due to luminous radiation. All evidence from this investigation and other investigations indicates that luminous radiation was insignificant. Heat transfer by nonluminous radiation from carbon dioxide and water vapor, on the other hand, was equal in magnitude to convective heat transfer; because of this, the nonluminous radiation can have a significant effect on cooling system design and performance.

## INTRODUCTION

The gas temperatures in high-performance turbojet-engine afterburners are generally much higher than the temperatures at which useful structural materials lose their strength. Therefore, the afterburner walls must be kept cool since heat is transferred to the afterburner walls or protective liners by forced convection and by radiation. Although no direct radiation measurements are known to have been made in an afterburner, the radiant heat transferred is believed to be both the nonluminous variety from carbon dioxide and water vapor and the luminous variety from carbon particles or other nongaseous substances in the exhaust. With certain conditions known, reasonable estimates of convective and nonluminous radiant heat transfer can be made (for example, ref. 1). Speculation on the existence of luminous radiation and the possibility that it might

intensify with increasing pressure level (see also ref. 2) prompted an investigation in a full-scale afterburner. This investigation, which was conducted at the NACA Lewis laboratory, is reported herein.

A turbojet engine was used as a gas generator for the afterburner. The engine inlet was connected to the laboratory air system in order that afterburner pressures considerably in excess of those attainable at sea-level static conditions could be obtained.

Orginally the investigation was to be conducted in two phases. The first phase consisted of a survey over the operating conditions of interes in order to define areas where detail measurements of emissivity should be made. Detail emissivity measurements were planned for the second phase of work. Only the first phase of work was completed since the results appeared largely negative. Data were obtained in order that the effect of pressure level on wall temperature could be directly observed and analyzed. Comparisons were made at a constant ratio of cooling airflow to afterburner gas flow. For a constant ratio of airflow to gas flow, the ratio of convective heat-transfer coefficients is essentially independent of pressure level, according to accepted correlations of heat-transfer data. Factors other than convective heat-transfer coefficients that affected wall temperatures were then easily isolated.

The results were interpreted in terms of results obtained in other investigations of luminous radiation from combustion flames (refs. 2 and 3). Afterburner-wall temperatures were obtained over a range of afterburner-outlet pressures from about 3700 to 6500 pounds per square foot absolute and an afterburner-outlet temperature of about 2840° F (3300° R).

## APPARATUS

### Afterburner

General features. - Construction features of the afterburner are shown in figure 1. The over-all length of the afterburner, exclusive of the exhaust nozzle, was 94.5 inches and it tapered from an inside diameter of 34.9 inches at the upstream end to 27.2 inches at the downstream end. A two-ring V-gutter flameholder was attached to the diffuser inner cone as shown in figure 2. The outer gutter was surrounded by a perforated screech-prevention shield similar to those described in reference 4. The screech shield was 10.0 inches long and extended 8.5 inches downstream of the flameholder-gutter trailing edge. The nature of this investigation made the use of an afterburner-wall inner-cooling liner (which has also been used as a screech suppressor) undesirable. A cooling liner would have prevented the control of some variables, such as cooling airflow, that are important in the interpretation of the results of the

investigation. At the same time, because of its erratic nature, screech could not be tolerated in a cooling investigation of the type that was conducted. The flameholder screech shield therefore appeared to be a good solution to the various requirements imposed.

Fuel for the afterburner was injected from 40 spray bars that were mounted on the inner cone and directed the fuel normal to the gas stream. The bars were arranged in two circumferential rows of 20 each at axial distances of 26.5 and 29.5 inches upstream of the leading edge of the flameholder. Spray bars at each of these axial positions were arranged in pairs, one behind the other. The pairs were located in longitudinal planes at 15° intervals around the circumference (four of these planes were occupied by the diffuser inner-cone support struts). Details of the fuel-spray-bar hole distribution are shown in figure 3.

Cooling system. - As shown in figure 1, about 38.5 inches of the afterburner wall were jacketed to form an annular cooling-air passage. Cooling air flowed through the annular passage from an annular header and was discharged radially at the downstream end of the passage. Cooling air was obtained from the laboratory compressed-air system and was directed normal to the afterburner axis into the header at two diametrically opposed points. The jacket and the header were insulated to prevent the convective flow of heat from the cooling air into the test cell. Figure 4 shows the afterburner both before (fig. 4(a)) and after (fig. 4(b)) the installation of the jacket insulation. One of the header air inlets is shown. Although the radial discharge slots for the cooling air are shown equipped with valves in figure 4(a), the valves and chain-drive mechanism were eventually abandoned and fixed discharge areas were used, as shown in figure 4(b). The three rectangular openings or windows through the jacket and afterburner wall shown in figure 4 were originally intended for direct measurement of radiation intensity. The windows were never used during the experimental program, however, because the initial results obtained indicated that luminous radiation was insignificant.

The significant geometrical characteristics of the cooling-air and the afterburner gas-flow passages are shown in figure 5. The annular cooling-air passage tapered from a depth of 0.88 inch at the upstream end to 0.58 inch at the downstream end. Within this same length the diameter of the afterburner gas flow passage tapered from 32.00 to 28.75 inches.

## Installation

The engine and afterburner were installed in a test cell that ran at approximately atmospheric pressure. High-pressure air from the laboratory air-supply system was ducted past regulating valves to both the engine inlet and the afterburner cooling system. A schematic diagram showing

the air-supply system for both the engine afterburner and the cooling-air system is shown in figure 6. The engine and afterburner were mounted on a free-floating thrust stand, which was balanced by a null-type air-pressure diaphragm. A labyrinth seal at the engine inlet was used to contain the high-pressure air supply and at the same time permit free axial movement of the thrust stand. A flexible bellows in the 16-inch line leading to the afterburner cooling jacket prevented the transmission of axial (thrust) forces from the cooling-air supply line to the thrust stand. The afterburner exhaust was discharged into a sound-suppression muffler at approximately atmospheric pressure and therefore required no exit-sealing provisions.

## Instrumentation

Afterburner-wall metal temperatures were measured at five longitudinal positions in the afterburner. These positions were designated stations A to E and varied in distance from 3.60 to 36.82 inches downstream of the flameholder. A tabulation of the specific distances for each station is given in figure 1. At each longitudinal station, thermocouples were installed at the top of the afterburner wall and at every $60^{\circ}$ position around the circumference.

Local gas temperature in the afterburner was measured at six longitudinal positions near the top centerline of the afterburner wall. These measurements were obtained with thermocouples that were shielded from thermal radiation. The shielded thermocouples were approximately 1/8 inch from the inside surface of the afterburner wall. Specific longitudinal and circumferential locations of these thermocouples are given in figure 1.

Cooling-air temperature measurements were taken inside the cooling-air passage at approximately the same longitudinal locations at which the afterburner-wall temperatures were measured. At each longitudinal location, measurements at several circumferential locations were taken.

The turbine-discharge or afterburner-inlet temperature was measured by six rakes spaced $60^{\circ}$ apart at a longitudinal station 39.09 inches upstream of the flameholder.

Engine airflow measurements were made at the engine inlet by a survey of total and static pressures and the temperature at the engine inlet. Afterburner cooling airflow was measured with a sharp-edged orifice (fig. 6). Fuel flows to the engine and to the afterburner were measured by calibrated rotating-vane electric flowmeters.

Afterburner-outlet total-pressure measurements were taken on a water-cooled diametrical rake just upstream of the exhuast nozzle (fig. 1).

## PROCEDURE

All data reported were obtained at nominally constant values of engine speed, turbine-outlet temperature (about 1150° F) and afterburner-outlet temperature. Afterburner-outlet pressure was varied by changing the pressure at the engine inlet. With the turbine-outlet and afterburner-outlet temperatures and the afterburner-outlet pressure set, the cooling airflow was varied between specified limits, and the data were obtained. The over-all range of cooling airflows covered was from 3.2 to 8.3 percent of the afterburner gas flow. The low cooling airflow limit was determined by the maximum allowable temperature for the afterburner wall, and the upper limit on cooling airflow was set by the maximum structurally allowable cooling-air pressure, which tended to collapse the afterburner walls inward. Data were obtained within these cooling airflow limits at five different afterburner-outlet pressures.

The fuel used in both the engine and the afterburner was JP-5.

## DISCUSSION OF RESULTS

Plots of wall temperature that are typical of the results obtained during the experimental investigation are shown in figure 7. Wall temperature at the 240° circumferential location for stations A to E is shown as a function of the ratio of the airflow rate through the annular cooling passage to the afterburner gas flow. The data shown in figure 7 are for runs during which the bulk gas temperature was close to 2840° F (3300° R). Separate plots are shown for afterburner-outlet pressures of 3680, 4275, 5190, 5885, and 6535 pounds per square foot absolute.

The trends shown in the curves of figure 7 are similar for all pressure levels as would normally be expected. The wall temperature decreases as the ratio of cooling airflow to gas flow increases because of an increasing ratio of the cooling-side convective heat-transfer coefficient to the gas-side heat-transfer coefficient. At a given ratio of cooling airflow to gas flow, the wall-temperature rise between stations A and B is significantly greater than the rise between other adjacent stations along the length of the afterburner. This peculiarity, which is noted at all five pressure levels, is believed to be caused by the partial thermal shielding of station A from nonluminous gas radiation by the screech shield surrounding the flameholder. This effect is discussed in more detail later.

The range of afterburner pressure level covered in this investigation had a slight effect on wall temperature. This effect is shown in figure 8 where the afterburner-wall temperature is plotted as a function of the afterburner-outlet pressure for stations A to E. Average curves have been drawn for each station. The data points shown for the curves were obtained

by cross-plotting the data from figure 7. These data points deviate from the curves in a consistent manner at all stations. The reasons for this deviation are not known; cross-plotting would be expected to yield smoother data-point trends than are shown, since no unusual scatter is evident in the basic data of figure 7. Small variations in setting the exhaust-gas bulk outlet temperature do not explain the deviations. The variation in exhaust-gas bulk outlet temperature was small and was random as can be seen in the tabulated values of figure 8. Inspection of other variables that might have affected the wall temperatures obtained at the various pressure levels did not yield any satisfactory explanation for the unusual data-point trend.

Despite the unusual data-point trends shown on figure 8, certain general trends are evident. At station A the wall temperature was substantially independent of pressure. At station B a slight pressure effect can be detected and progressively greater effects are noted with the increasing distance downstream along the burner wall. At station E the wall temperature increased by about $180^{\circ}$ F as the afterburner-outlet pressure increased from 3700 to 6500 pounds per square foot absolute.

The curves shown in figure 8 are for a fixed ratio of cooling airflow to gas flow. At each station the ratio of convective heat-transfer coefficients on the gas and cooling-air surfaces of the afterburner wall would be essentially independent of pressure. Any variation of wall temperature with pressure should therefore be attributable to increasing radiant heat transfer (relative to convective heat transfer) or to increasing temperature of the gas layer adjacent to the wall.

The curves shown in figure 9 strongly suggest that the changes in wall temperature with pressure were primarily due to changes in local gas temperature. In figure 9 the wall temperature at station E and the locally measured gas temperature adjacent to the wall at the same longitudinal station are plotted against afterburner-outlet pressure. A marked rise in local gas temperature with increasing afterburner pressure is evident. Analysis showed that the convective heat-transfer coefficients on the cooling and gas sides of the wall were approximately equal for the operating conditions given for figure 9. Thus, the wall temperature rise should be half as great as the local gas-temperature rise. Inspection of the wall temperatures shows that this is approximately the case.

The results obtained in the investigation of reference 2 suggest that if luminous radiation in the afterburner were significant, a much more pronounced variation in wall temperature with pressure would have been observed, particularly at the upstream stations. The investigation reported in reference 2 employed a primary combustor from a turbojet engine. Direct radiation measurements near the upstream end of the burner showed a high level of gas emissivity that increased markedly with increasing pressure. This was attributed to luminous radiation from soot

particles. Toward the downstream end of the combustor, where the soot was consumed, gas radiation was found to be insignificant.

In another investigation (ref. 3) direct measurements of radiation were made at various longitudinal positions in a furnace-type burner. The burner was operated with both gaseous and liquid fuels. In the upstream portions of the burner where free carbon could form with the heavy-oil type fuels, a high level of luminous radiation was observed. Near the downstream end of the burner, where the particles were consumed, the radiation level approached that for nonluminous radiation from carbon dioxide and water vapor present in the combustion gas. The gaseous-type fuel used in the experiments of reference 3 gave a radiation level corresponding to nonluminous radiation from carbon dioxide and water vapor over the entire length of the burner.

It is unlikely that much free carbon is formed in an afterburner where the fuel and the air enter the combustion zone in a premixed vaporized state and deliberate efforts are made in the interest of efficient operation to avoid local fuel-air ratios much in excess of a stoichiometric mixture. Observations of the flame emerging from the exhaust nozzle tend to confirm this. The flame was light blue with no traces of the yellow that is characteristic of fuel-rich flames. Therefore, luminous radiation likely did not contribute much to wall heating in the afterburner, and whatever level of luminous radiation that might have been present did not vary with pressure, as is evident in figure 8.

On the other hand, nonluminous radiation from the afterburner gases constituted a very significant part of the total heat transferred through the afterburner walls. This fact can be deduced from the curves that are shown in figure 10. In this figure the longitudinal distribution of wall temperature for a typical run is shown. Two wall-temperature curves are shown: one experimental and one calculated for the wall temperature that would be expected if the heat transferred to the wall was due to forced convection only. The local gas temperature near the afterburner wall is also shown for reference.

The experimental wall-temperature curve in figure 10 shows a relatively regular increase from station B to station E. The increase is caused primarily by the increasing local temperature near the afterburner wall. The measured temperature at station A, however, is from $100^{\circ}$ to $120^{\circ}$ F lower than would be expected if the established curve for station B to E were extrapolated to station A in a reasonable manner. This decrease in temperature at station A is attributed to the partial thermal shielding of station A from nonluminous gas radiation by the screech shield that surrounded the flameholder.

The intensity of nonluminous radiation from the afterburner gases can be visualized by comparing the computed wall-temperature curve with

the experimental curve. The experimental and computed temperature curves are similar in trend except in the region of station A for the reasons previously noted. At station A the measured and computed wall temperatures are approximately 100° F different. About half this temperature difference can be accounted for by including radiation from the screech shield metal to station A.

An estimate of the nonluminous radiant heat transfer of the gases to the wall was made for station E in the afterburner where it was felt that conditions were well enough defined to permit estimation. The radiant heat transfer from the gases to the afterburner walls was about equal to the convective heat transfer and the wall at station E was from 210° to 280° F hotter than the value predicted from convective heat transfer alone. This is in fair agreement with the observed wall temperature. The estimated magnitude of radiant heat transfer that is accepted depends upon the choice of an uncertain correction for the fact that the afterburner walls have an emissivity less than 1.0. The methods used in the calculation of nonluminous radiant heat transfer are given in the appendix.

Shielding from gas radiation was previously used as an explanation for the peculiar results of the wall-temperature measurements at station A. Also, there is an inference in the comparison of the curves of figure 10 that the contribution of nonluminous radiant heat transfer was roughly constant along the length of the afterburner. This could easily be the case. Although the bulk temperature or average temperature of the gases decreases with distance upstream toward the flameholder, local temperatures in some regions of the flame are near stoichiometric mixture temperature (over 3600° F). (Fuel-air-ratio surveys for this afterburner configuration showing this to be the case are presented in fig. 9 of ref. 4.) In this range of temperatures, radiation intensity varies approximately as the cube of the absolute temperature when changes in gas emissivity are accounted for. This variation in radiation intensity could offset the diminishing mass from which gas radiation occurs in the upstream parts of the burner.

## CONCLUDING REMARKS

An investigation was conducted to determine the effect of pressure level on afterburner-wall temperatures. It had been anticipated prior to the investigation that luminous radiation might constitute a significant part of the total heat transferred to the afterburner walls. It was also felt that luminous radiation, if present, might intensify with increasing pressure.

The results obtained in this investigation indicated that heat transfer by luminous radiation was not significant at any pressure level investigated (from 3700 to 6500 lb/sq ft abs). When the ratio of

afterburner-wall cooling airflow to afterburner gas flow was constant, the wall temperature increased with pressure. The increased wall temperatures were due to higher local gas temperatures near the wall, which led to higher rates of convective heat transfer.

Nonluminous radiation from carbon dioxide and water vapor in the afterburner was important. In one case that was analyzed, the heat transferred by nonluminous radiation was about equal to the heat transferred by forced convection.

Lewis Flight Propulsion Laboratory
National Advisory Committee for Aeronautics
Cleveland, Ohio, April 7, 1958

## APPENDIX - WALL TEMPERATURE CALCULATIONS

### Symbols

The following symbols are used in the calculations:

| | |
|---|---|
| $A$ | area of afterburner wall |
| $h_a$ | convective heat-transfer coefficient on cooling-air side of afterburner wall, Btu/(sec)(sq ft)($^\circ$R) |
| $h_g$ | convective heat-transfer coefficient on gas side of afterburner wall, Btu/(sec)(sq ft)($^\circ$R) |
| $T_a$ | cooling-air temperature, $^\circ$R |
| $T_g$ | gas temperature, $^\circ$R |
| $T_w$ | wall temperature, $^\circ$R |
| $q/A$ | radiant heat transfer per unit area of afterburner wall, Btu/(sq ft)($^\circ$R) |
| $\alpha_g$ | afterburner gas absorptivity |
| $\varepsilon_g$ | afterburner gas emissivity |
| $\sigma$ | Stefan-Boltzmann constant, $0.1713\times10^{-8}$ Btu/(hr)(sq ft)($^\circ$R)$^4$ |

### Calculations

If the thermal resistance of the metal walls is negligible compared with the convective heat-transfer coefficients on the afterburner-gas and cooling-air sides of the wall, the wall metal temperature may be obtained from

$$T_w = \frac{T_g + \frac{h_a}{h_g} T_a}{1 + \frac{h_a}{h_g}}$$

when heat is transferred to the wall by forced convection only.

When estimates were made of the wall temperature that would result from convective heat transfer, the local measured values of gas temperature near the wall were used. Average cooling-air temperatures within

the cooling passage at a given station were used. Heat-transfer coefficients were obtained by using equation (9-32C) of reference 5 (p. 242).

If, in addition to convection, heat is also transferred to the walls by radiation, the wall temperature may be obtained from

$$T_w = \frac{\frac{q}{A}}{h_a + h_g} + \frac{T_g + \frac{h_a}{h_g} T_a}{1 + \frac{h_a}{h_g}}$$

As noted previously, an estimate of the magnitude of nonluminous radiation from water vapor and carbon dioxide was made for station E at one operating condition. This estimate was made according to the methods of reference 5 (pp. 82 to 91). Reference 5 gives two equations that may be used to obtain the value of $q/A$ for nonluminous radiation. Of these, the simplest for the purposes of this report was, in modified form,

$$\frac{q}{A} = \frac{\sigma}{3600} (\varepsilon_g T_g^4 - \alpha_g T_w^4)$$

which is given as equation (4-57) in reference 5. This equation is for a black receiver with an emissivity of 1.0. For receivers with emissivities less than 1.0, a correction factor must be applied as noted previously in this report and subsequently in this section.

The problem of estimating $q/A$ is primarily a matter of determining the emissivity of the gas. The gas emissivity depends upon the temperature of the gas, the partial pressure of each of the radiating gases present, the total pressure of the gas mixture, and a geometrical factor called beam length, which accounts for the total depth of the gas from which emission takes place (in contrast to radiation from opaque substances in which the emission is essentially from the surface). For the run that was analyzed in this report, the total pressure of the afterburner gas mixture was 2.46 atmospheres. At a fuel-air ratio of 0.0467, the partial pressures of carbon dioxide and water vapor were 0.248 and 0.258 atmosphere, respectively. The beam length was assumed to be 0.9 of the afterburner diameter (see table 4-2 of ref. 5) at station E. This gave a beam length of 2.18 feet. The total temperature of the gas was $3272^{\circ}$ R as given on figure 10. These factors gave an estimated gas emissivity of 0.211.

The gas absorptivity $\alpha_g$ is dependent upon the factors that determine emissivity and also upon the wall temperature. For the cases analyzed, the wall temperature to the fourth power was small compared with the fourth power of the gas temperature. This difference allowed the simplification

(with a very small error) of assuming that the gas absorptivity was equal to the emissivity.

For the example in figure 10, the calculated black-receiver value of q/A was 10.9 Btu per second per square foot. If this value of q/A is multiplied by 0.6 (the emissivity of burned Inconel) the effective value of q/A would be 6.54 Btu per second per square foot. The sum $h_a + h_g$ for this example was estimated to be 0.031 Btu per second per square foot per $^{\circ}R$ so that the wall-temperature difference due to radiant heat transfer would be $210^{\circ}$ F. If the multiplying factor is chosen as the average between the emissivity of 0.6 and a perfect black body (see ref. 5, p. 91) the wall-temperature difference due to radiant heat transfer would be $280^{\circ}$ F.

## REFERENCES

1. Koffel, William K., and Kaufman, Harold R.: Investigation of Heat-Transfer Coefficients in an Afterburner. NACA RM E52D11, 1952.

2. Topper, Leonard: Radiant Heat Transfer from Flames in a Single Tubular Turbojet Combustor. NACA RM E52F23, 1952.

3. Sherman, R. A.: Heat Transfer by Radiation from Flames. ASME, Paper No. 56-A-111, 1956.

4. Trout, Arthur M., Koffel, William K., and Smolak, George R.: Investigation of Afterburner Combustion Screech and Methods of Its Control at High Combustor Pressure Levels. NACA RM E55K25, 1956.

5. McAdams, William H.: Heat Transmission. Third ed., McGraw-Hill Book Co., Inc., 1954.

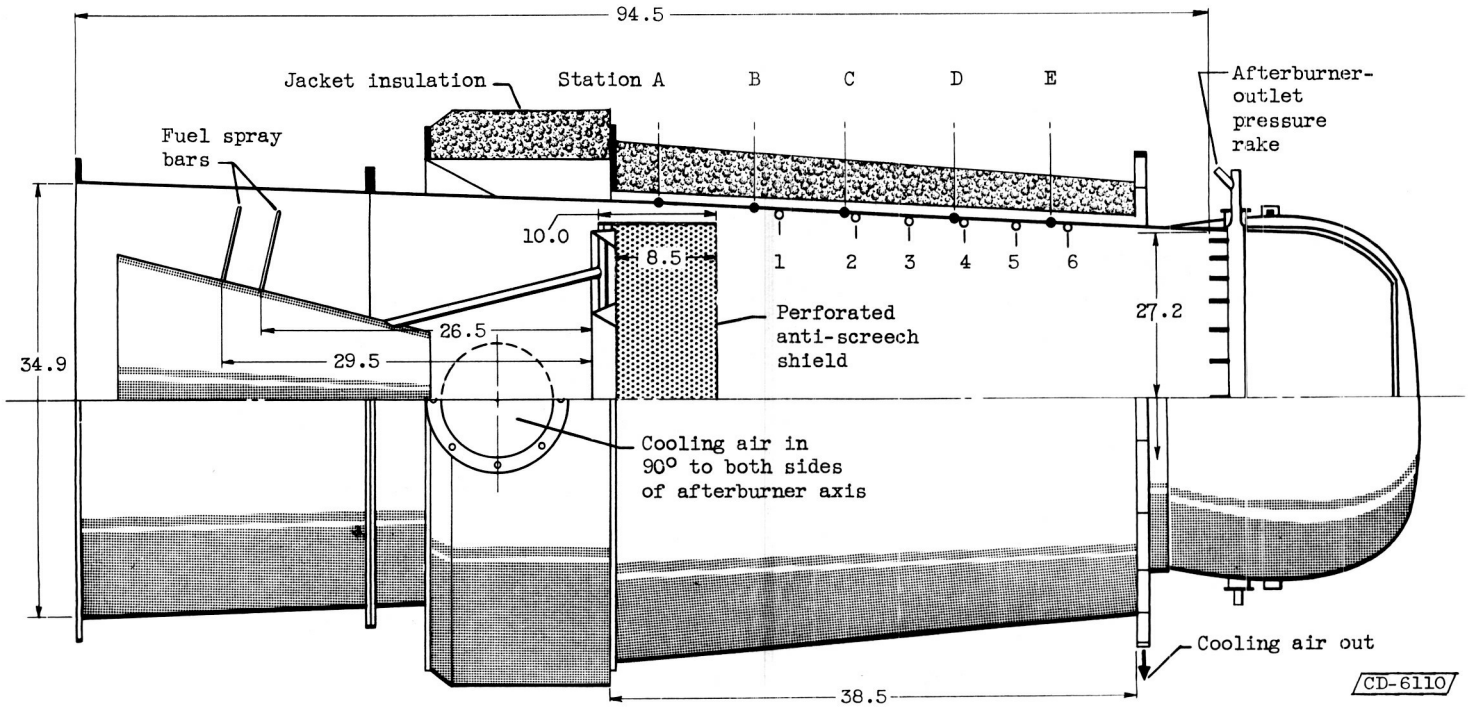


● Wall thermocouple (metal temperature)

o Shielded thermocouple 1/8 in. from wall (gas temperature)

| Station | Distance downstream of flameholder, in. | Temperature | Circumferential location, deg |
|---|---|---|---|
| A | 3.6 | Wall | 0, 60, 120, |
| B | 11.82 | | 180, 240, 300, |
| C | 19.44 | | typical for all |
| D | 29.01 | | stations |
| E | 36.82 | | |
| 1 | 13.94 | Gas | 22 |
| 2 | 20.44 | | 20 |
| 3 | 24.74 | | 17 Clockwise |
| 4 | 29.44 | | 15 downstream |
| 5 | 33.94 | | 12 |
| 6 | 38.44 | | 10 |

Figure 1. - Afterburner details. (All dimensions in inches.)

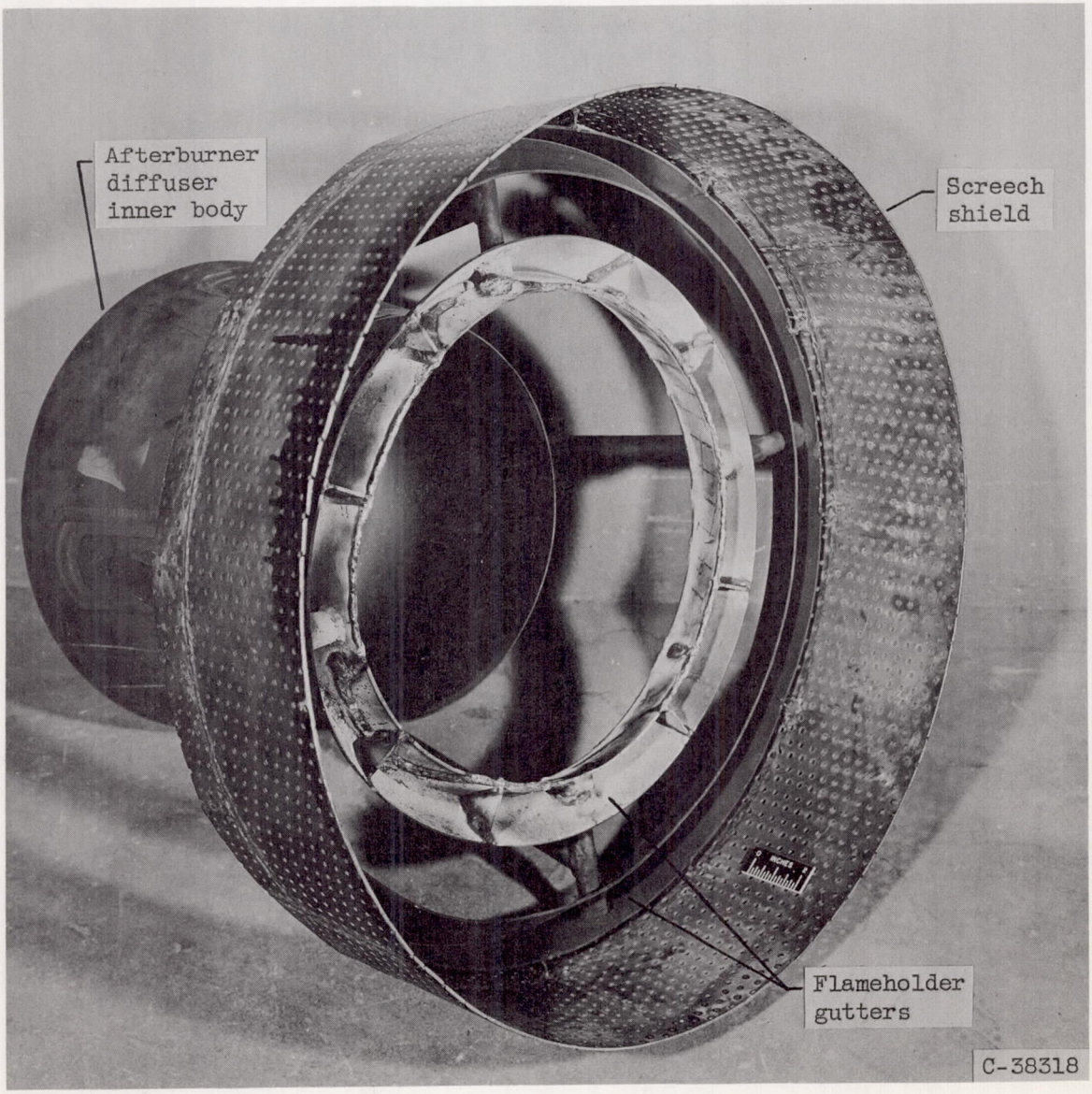


Figure 2. - Flameholder and screech shield.

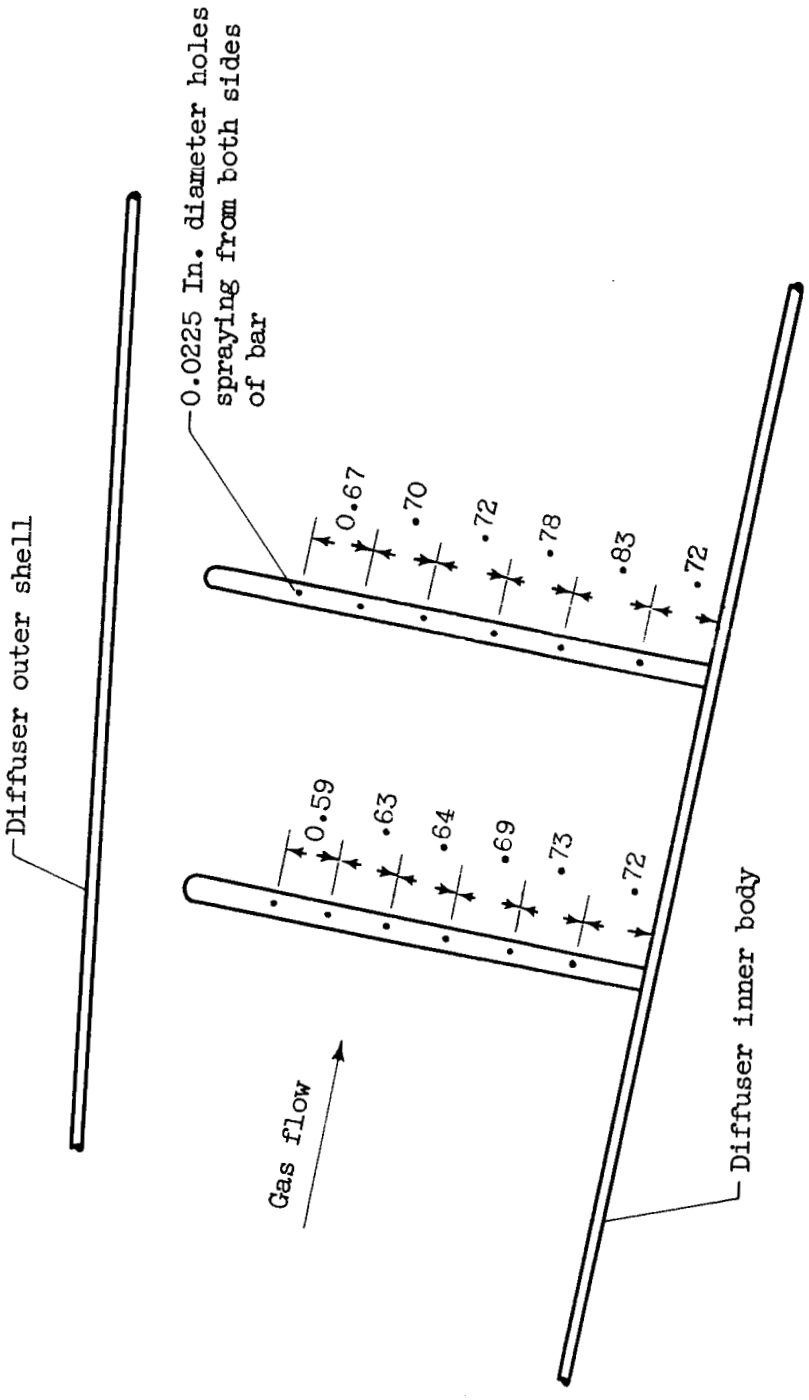


Figure 3. - Fuel-spray-bar hole distribution. (All dimensions in inches.)

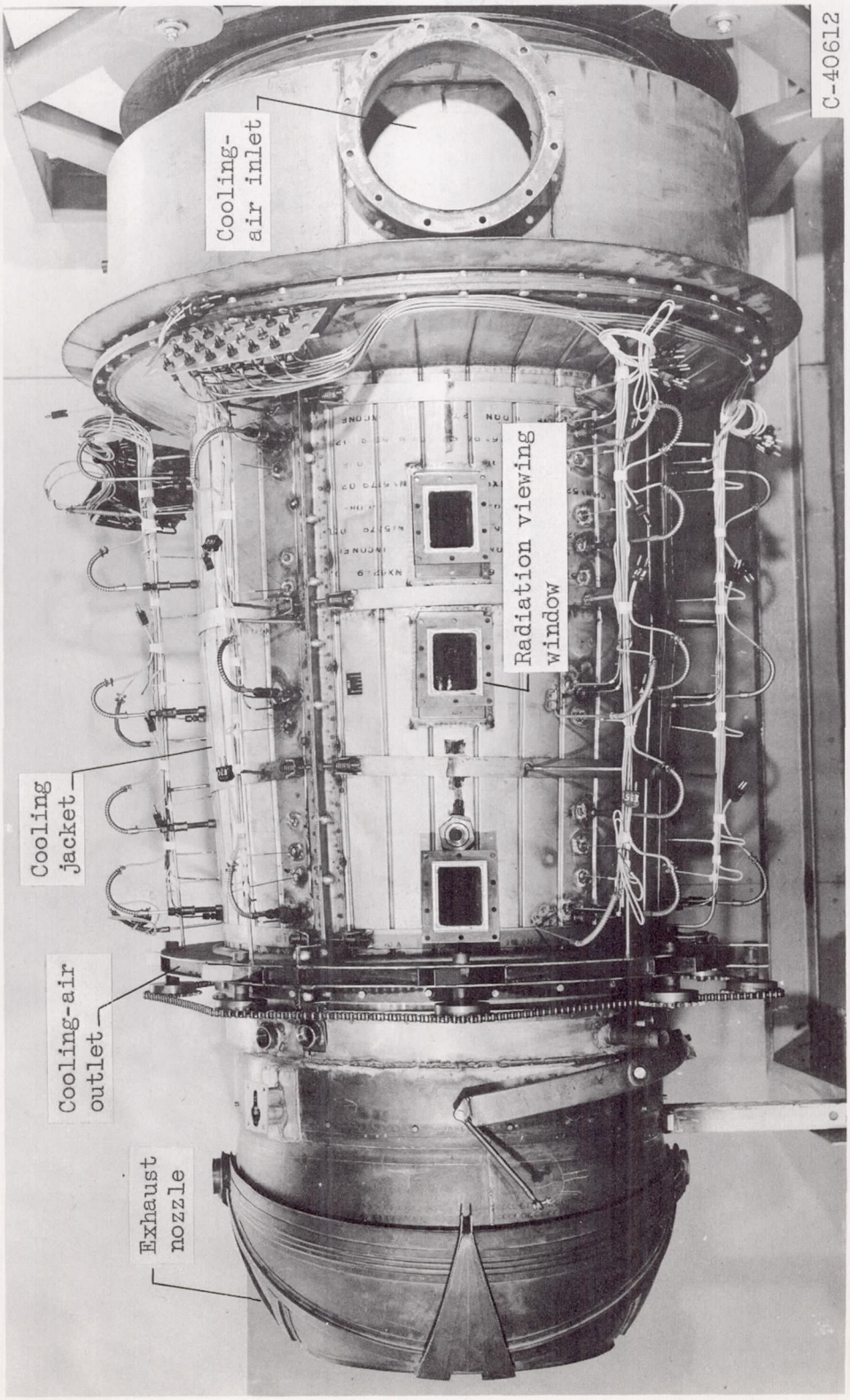


(a) Before installation of insulation.

Figure 4. - Afterburner.

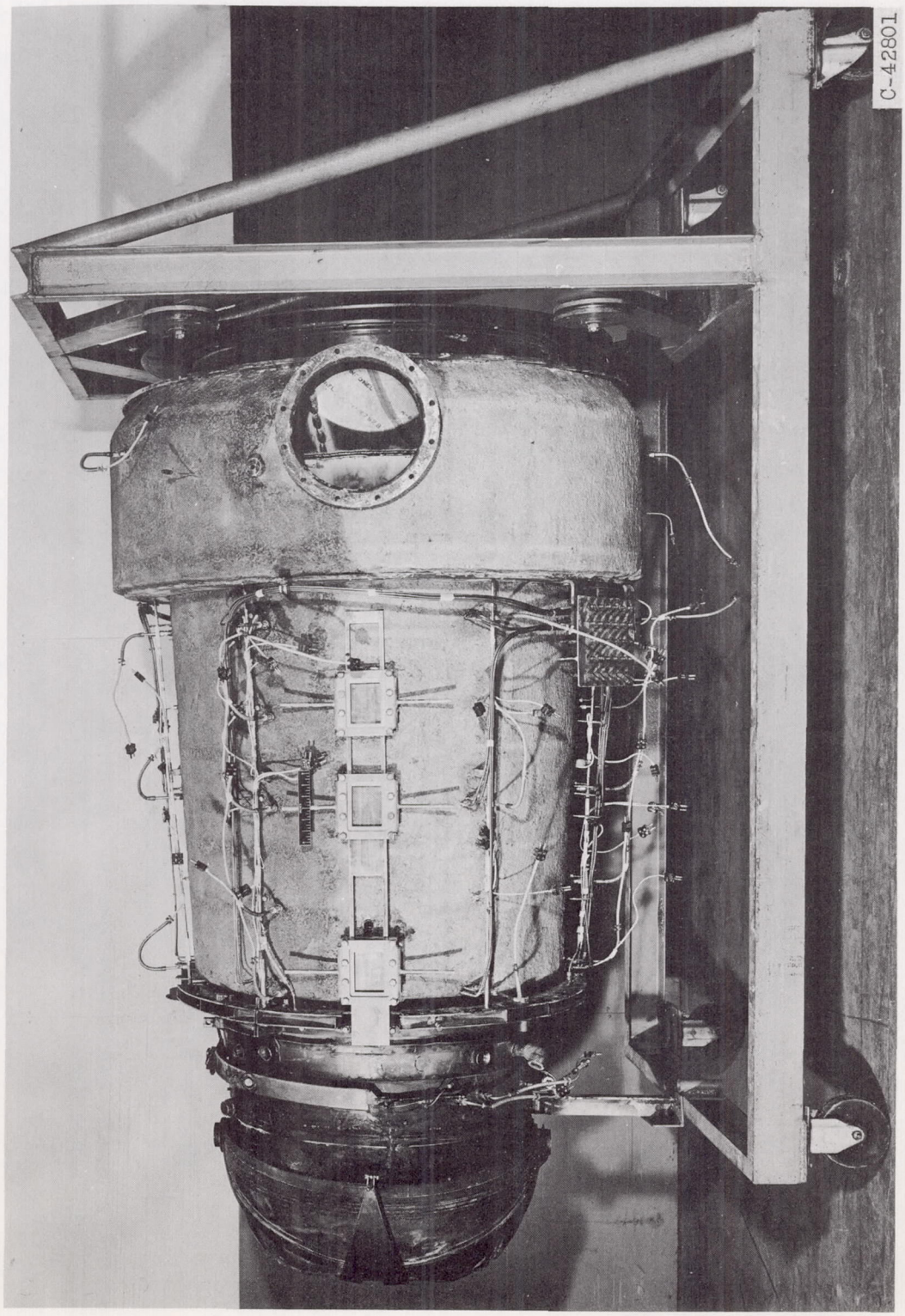


(b) After installation of insulation.

Figure 4. - Concluded. Afterburner.

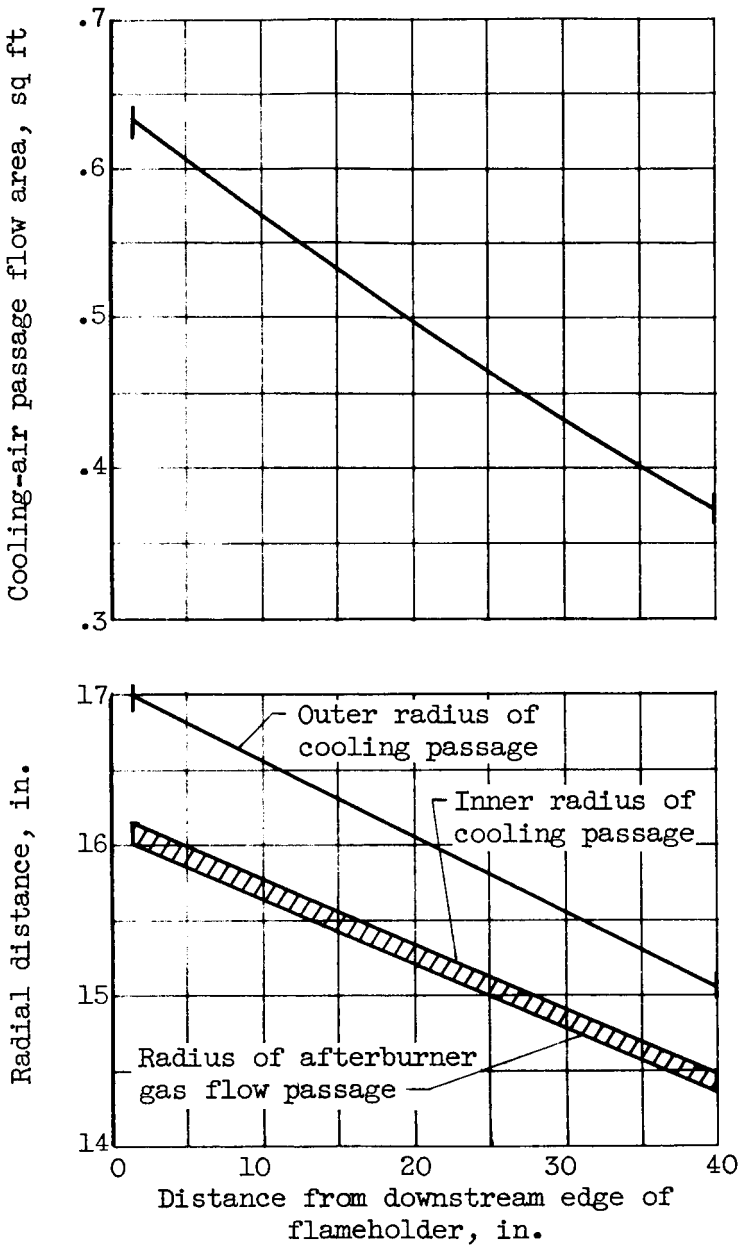


Figure 5. - Geometrical characteristics of cooling-air and afterburner gas flow passages.

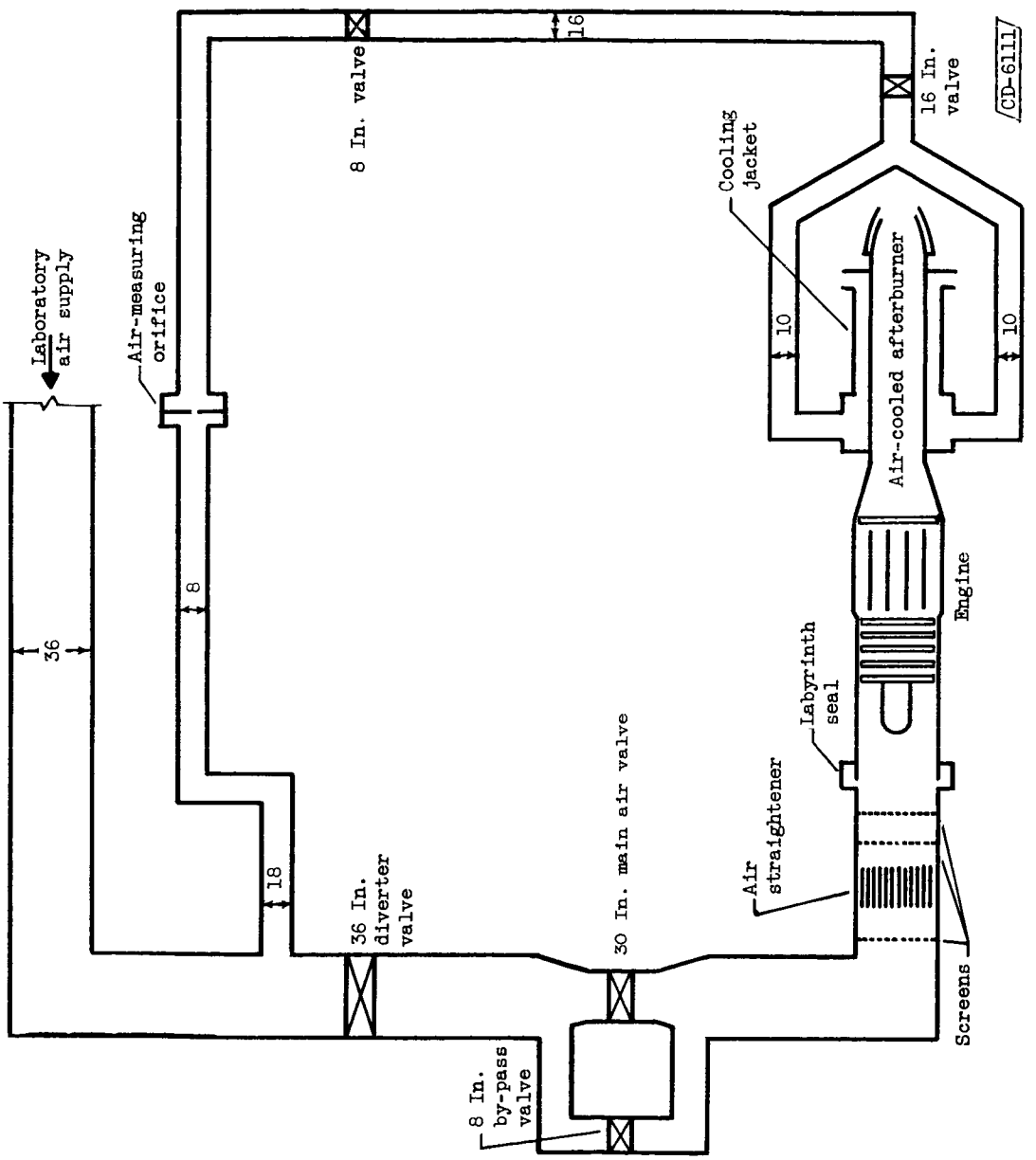


Figure 6. - Schematic diagram of air supply system for engine and afterburner cooling jacket. (All dimensions in inches.)

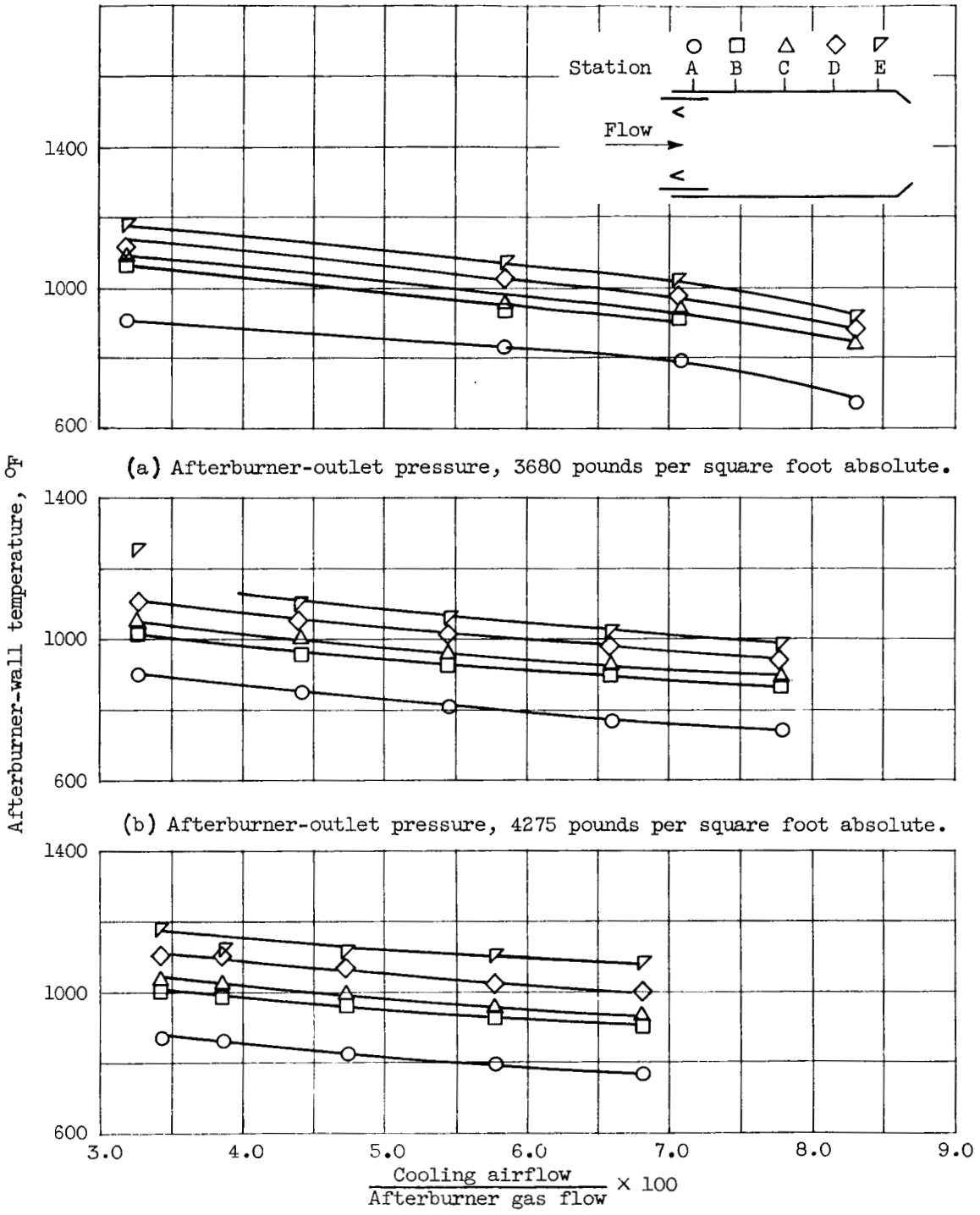


(a) Afterburner-outlet pressure, 3680 pounds per square foot absolute.

(b) Afterburner-outlet pressure, 4275 pounds per square foot absolute.

(c) Afterburner-outlet pressure, 5190 pounds per square foot absolute.

Figure 7. - Variation of afterburner-wall temperature with cooling airflow at 240° circumferential location. Afterburner-outlet bulk temperature, approximately 2840° F (3300° R).

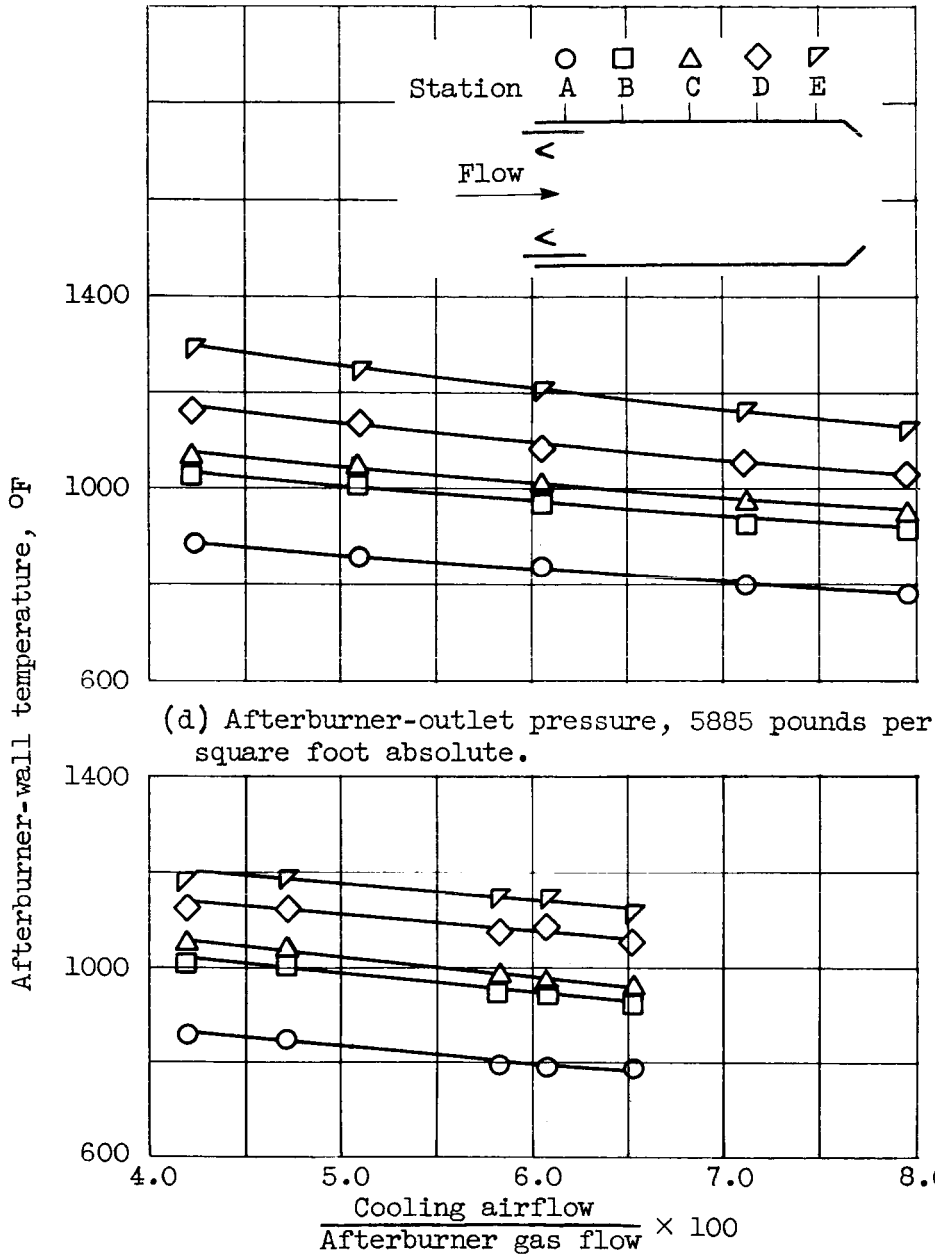


(d) Afterburner-outlet pressure, 5885 pounds per square foot absolute.

(e) Afterburner-outlet pressure, 6535 pounds per square foot absolute.

Figure 7. - Concluded. Variation of afterburner-wall temperature with cooling airflow at 240° circumferential location. Afterburner-outlet bulk temperature, approximately 2840° F (3300° R).

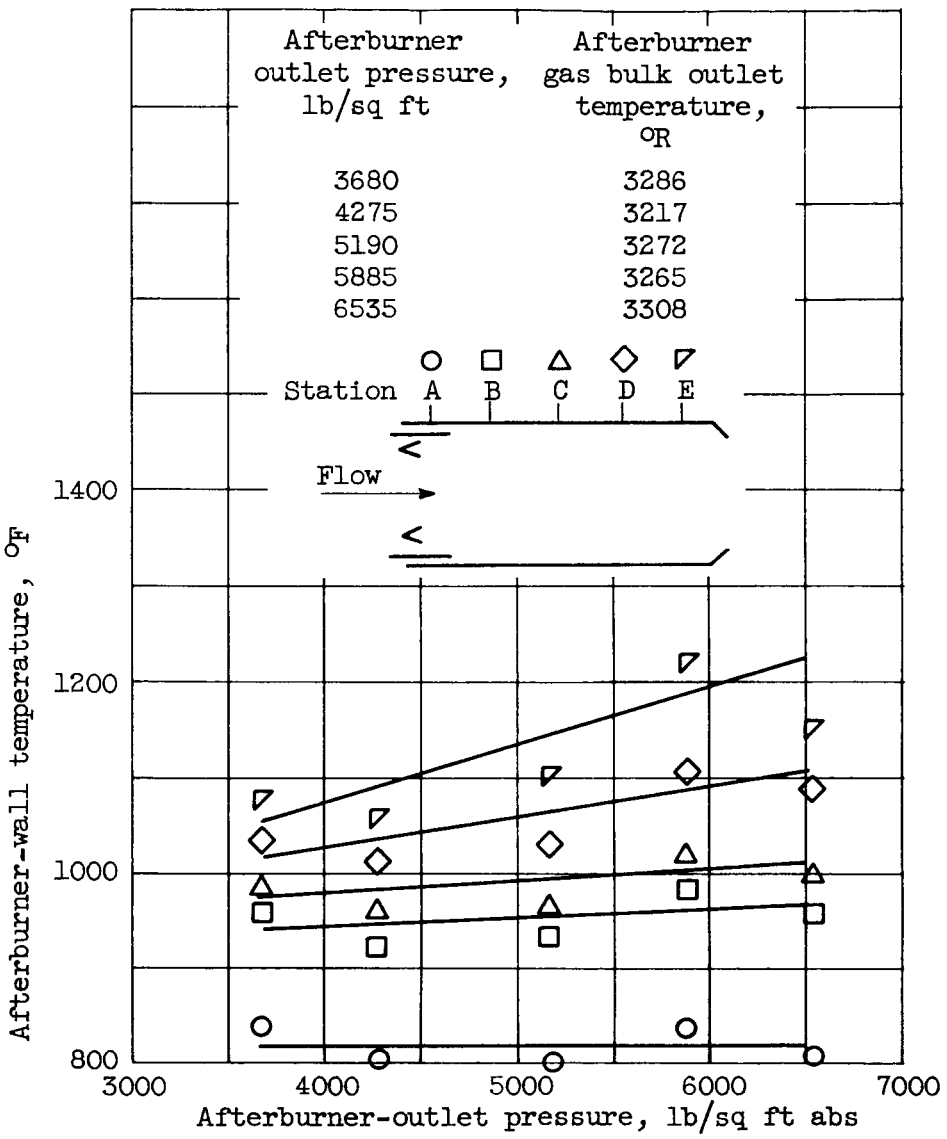


Figure 8. - Effect of afterburner pressure on afterburner-wall temperature. Cooling airflow equal to 5.75 percent of afterburner gas flow. Circumferential location, 240°.

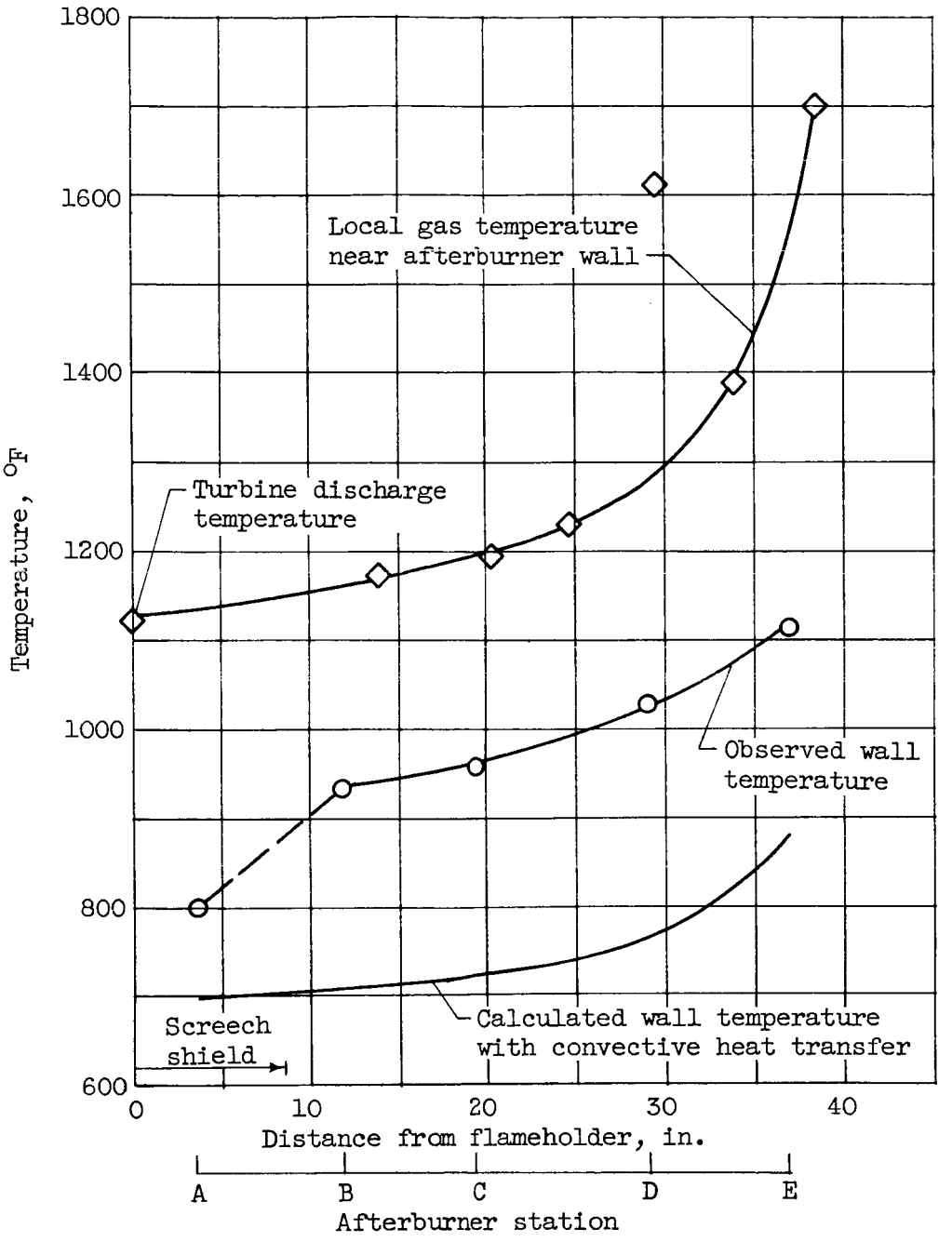


Figure 10. - Longitudinal variation of afterburner-wall temperature. Cooling airflow equal to 5.72 percent of afterburner gas flow; afterburner-outlet temperature, 2812° F (3272° R); afterburner-outlet pressure, 5202 pounds per square foot absolute.



NACA - Langley Field, Va.

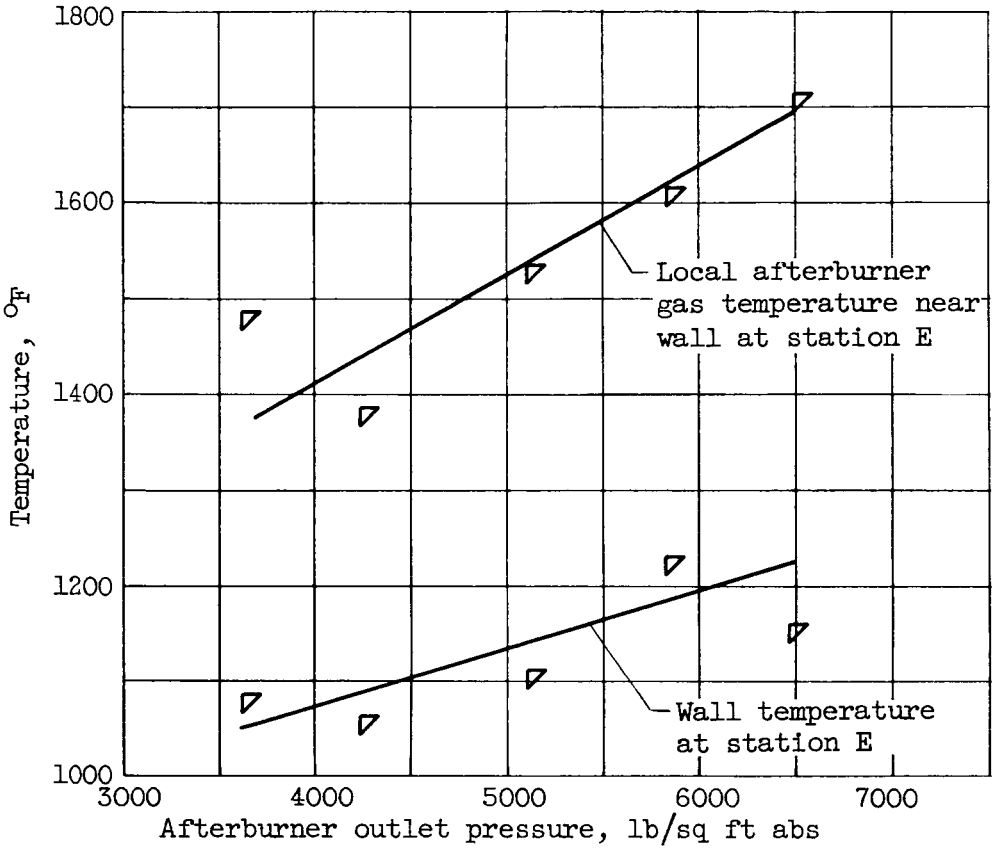


Figure 9. - Effect of pressure on afterburner-wall temperature and local gas temperature at station E. Cooling airflow equal to 5.75 percent of afterburner gas flow. Afterburner gas bulk outlet temperature, approximately 2815° F (3275° R).

UNCLASSIFIED